BMC Research Notes

RESEARCH NOTE

Open Access

Comprehensive insights into sepsis-induced cardiac dysfunction through proteomics and metabolomics

Heyu Ji[1], Ting Xiao[1], Peijun Li[2], Junmei Xu[1*] and Yulong Cui[1*]

Abstract

Objective Sepsis remains a leading cause of mortality worldwide, with cardiac dysfunction contributing substantially to sepsis-related deaths. Due to the unique biology of myocardial tissue, the mechanisms underlying sepsis-induced cardiac injury are incompletely understood. This exploratory study aimed to apply integrated proteomic and metabolomic profiling to characterize molecular alterations in cardiac tissue from a cecal ligation and puncture mouse model of sepsis.

Results Comparative analysis identified 118 significantly altered proteins (75 upregulated and 43 downregulated) and 190 significantly altered metabolites (174 upregulated and 16 downregulated). Integrated pathway and network analyses implicated biological processes including platelet activation, mineral absorption, drug metabolism, terpenoid backbone biosynthesis, and butanoate metabolism. Notably, several previously under-recognized proteins (Prpsap1, Qsox1 and Prph), were identified as differentially expressed and ranked highly in our integrated network analyses, while prostaglandin H2, prostaglandin I2, thromboxane A2 and L-glutamine emerged as central metabolic nodes. These data extend the molecular landscape of septic cardiomyopathy and nominate prioritized candidates for orthogonal validation and mechanistic study.

Keywords Sepsis, Cardiac dysfunction, Proteomics and metabolomics, Novel biomarker

Introduction

Sepsis is a systemic inflammatory response syndrome and a worldwide healthcare issue, which leads to a life-threatening multiple organ dysfunction if not treated promptly [1, 2]. According to the national figures, nearly 270,000 deaths out of 1.7 million cases of sepsis are reported each year, with a high mortality rate and massive expenses for treatments [3]. Sepsis is also a dysregulated host response to infection involving various organs, with cardiac dysfunction being particularly critical for patient outcomes [4]. Up to 50% mortality rate is associated with septic cardiomyopathy, its pathogenesis involves a complex interaction between chemical mediators and mitochondrial dysfunction [5, 6]. Septic cardiomyopathy, commonly

*Correspondence:
Junmei Xu
13975148864@139.com
Yulong Cui
cuiyulong@csu.edu.cn
[1]Department of Anesthesiology, The Second Xiangya Hospital, Central South University, Changsha 410011, Hunan, People's Republic of China
[2]Department of Anesthesiology, Shenzhen Baoan Women's and Children's Hospital, Jinan University, Shenzhen 518102, Guangdong, China

known as sepsis-induced cardiomyopathy (SICM), is caused by sepsis. It is defined by cardiac collapse that occurs rapidly and transiently and subsequent circulation abnormalities, are perhaps the most often diagnosed symptoms in people with sepsis [7]. SICM is frequently observed in patients suffering from sepsis, however, its incidence is often underreported due to limitations in technical constraints [8]. Despite its clinical significance, the precise molecular mechanisms underlying SICM remain largely unknown, highlighting a critical knowledge gap regarding cardiac tissue in sepsis [9].

Omics technology could aid in investigating pathophysiological processes, identifying biomarkers, molecular profiling, and characterizing complicated biochemical systems [10]. Proteomics and metabolomics show the dynamic alterations that occur after genomics and transcriptomics have taken place. The proteome is a database of all the proteins and peptides found in tissues. The metabolic profile reveals changes in metabolic and metabolites pathways occurring in the body under various situations. To completely understand the physiologic activity, single omics are insufficient. Combining metabolomics and proteomics can provide an even more thorough overview of physiological status, especially in terms of understanding etiology and discovering biomarkers, employing modern data analytic skills to analyze the complex system in its entirety.

The goal of this study was to develop a more complete understanding of the molecular pathways of septic cardiomyopathy by doing an integrated proteome and metabolomics analysis on a SICM mouse model. Thus, we investigated the fundamental alterations in the metabolome and proteome of septic mouse cardiac tissues. This illustrates the critical nature of understanding the relative metabolite abundances and protein expression patterns using LC-MS to determine the representative changes associated with the development of cardiomyopathy in response to sepsis.

Experimental procedures

For animal proteomic and metabolomic analysis, animal models were performed and analyzed in replicated of 3 and 6, respectively, for each of two conditions (with CLP and control surgery). We created an interactive volcanic map and a hierarchical clustering chart utilizing the R program.

Experimental animal model

Following approval by the Institutional Animal Care and Use Committee at The Second Xiangya Hospital, C57BL/6J mice (aged 6–8 weeks, male) were purchased from the SLAC experimental animal center (Changsha, China). State and institutional norms and regulations were followed for all animal requisitions, housing, treatments, and procedures.

As described earlier by Chaudry et al., a model of sepsis was created via CLP (Supplementary methods) [11]. At 24 h post-surgery (the designated endpoint), the mice were deeply anesthetized with sevoflurane (1.5-2% in oxygen) until loss of reflexes was confirmed. While under anesthesia, the thoracic cavity was aseptically opened and the heart was carefully excised. This procedure led to immediate death and irreversible cessation of circulation. This approach is recognized as a humane and approved method of euthanasia, consistent with the American Veterinary Medical Association (AVMA) guidelines for the euthanasia of animals. Residual blood was gently removed by rinsing in pre-cooled sterile phosphate-buffered saline (PBS) to minimize contamination. The whole heart was dissected under sterile conditions and immediately snap-frozen in liquid nitrogen to preserve protein and metabolite integrity. Samples were stored at -80 °C until further processing.

Echocardiography

Sevoflurane inhalation was used to induce light anesthesia. An ultrasound (VINNO 8), a mechanical transducer with a 30 Hz center frequency and a 30 Hz frame rate, was used for the echocardiography. Measurements of the Left Ventricular End-Diastolic Diameter (LVEDd) and Left Ventricular End-Systolic Diameter (LVESd) were performed, accompanied by evaluations of the Ejection Fraction (EF) and Fractional Shortening (FS) to assess ventricular function. Analyses were conducted using the averaged values from three cardiac cycles of measurements.

Hematoxylin-eosin (HE) staining

After 24 h in a 4% neutral formaldehyde fixator, cardiac tissue samples were rinsed with water and dried. Following dehydration, the tissue samples were embedded in paraffin. For histological analysis, sections of paraffin-embedded tissue were cut into 5 μm sections and stained with HE.

Enzyme-linked immunosorbent assay (ELISA)

At 24 h of post-surgery, blood samples were taken and centrifuged for serum separation. The contents of creatine kinase-MB (CK-MB), lactate dehydrogenase (LDH) and cardiac troponin-T (cTnT) were detected through a high-sensitivity cardiac enzyme-linked immunosorbent assay kit (USCN Life Science, Wuhan, China) following the manufacturer instructions. A microplate reader measured the absorbance at 450 nm (OD450).

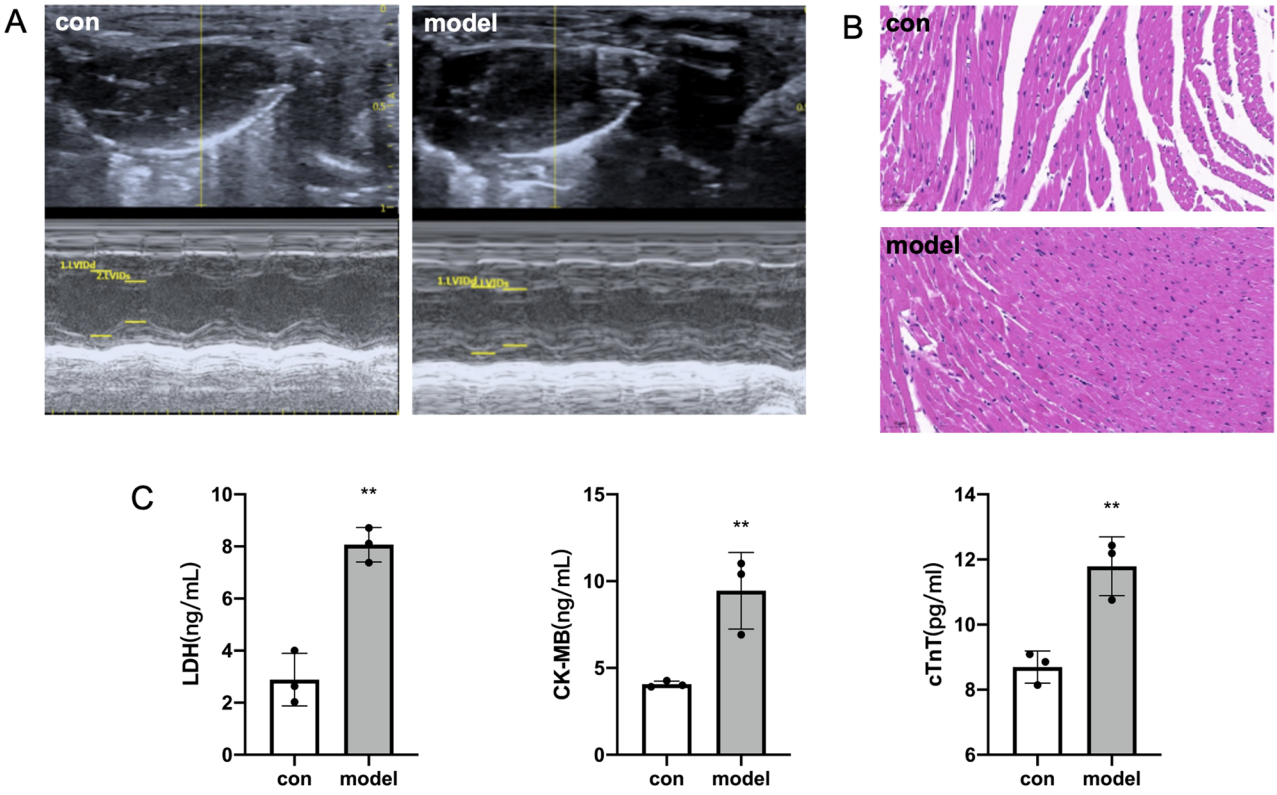

Fig. 1 Shows how to identify and analyze septic cardiomyopathy. **A** Displays the echocardiography imaging obtained after CLP surgery. M-mode (parasternal short axis) and B-mode (parasternal long and short axis) pictures were collected after 24 h following CLP surgery. **B** Hematoxylin and eosin (HE) stained slices of cardiac tissues. These HE slices were taken from mouse heart tissues after 24 h following CLP surgery. The CLP group represent the necrotic region of the myocardial tissue (400× magnification power for all recorded images). **C** Serum levels of CK-MB, LDH, and cTnT were measured 24 h after CLP procedure. *$P < 0.05$ for CLP vs. Control

Proteomics and metabolomics analysis

Proteomic analyses were conducted using 3 biological replicates, and metabolomic analyses using 6 biological replicates, each derived from independent samples. Comprehensive methodological details, including instrument parameters, quality control pipelines, and data processing settings, are provided in the Supplementary Methods.

Statistical analysis

Statistical analyses were conducted using GraphPad Prism version 8.0, and R program. Differentially expressed proteins and metabolites were identified using univariate t-tests combined with Benjamini-Hochberg false discovery rate (FDR) correction to control for multiple comparisons. Multivariate analyses, including PCA and PLS-DA, were employed to assess global variation patterns and complement univariate findings. Data are presented as mean ± SEM. We created an interactive volcanic map and a hierarchical clustering chart utilizing the R program. To determine statistical significance, we employed the t-test, and $P < 0.05$ was considered significant.

Table 1 Echocardiographic parameters comparing control and CLP groups

	Control	CLP	*P* valve
LVEF(%)	64.20 ± 3.68	44.26 ± 13.49	0.0058**
LVFS(%)	29.99 ± 2.59	18.81 ± 6.89	0.0040**
LVEDd(mm)	3.56 ± 0.12	2.95 ± 0.22	0.0001***
LVESd(mm)	2.490 ± 0.04733	1.70 ± 0.56	0.0059**
SV(uL)	71.67 ± 11.69	75.00 ± 5.48	0.5413
HR(bpm)	347.8 ± 31.91	345.3 ± 49.92	0.9197

Results

Identifying the model of septic cardiomyopathy

Our findings show that the CLP model had no significant effect on body weight. Using echocardiography, we found that the CLP model enhanced LVESd, decreased fractional shortening, and had minimal effect on LV wall thickness, LVEDd, and LV mass (Fig. 1A). This is consistent with prior investigations [12]. Table 1. summarizes the echocardiographic measurements of left ventricular function and structure in the control and CLP groups. Key parameters include LVEF, LVFS, LVEDd, and LVESd. LVEF and LVFS were significantly reduced in the model group compared to the control group ($P < 0.01$), indicating impaired systolic function. Structural parameters,

including LVEDd and LVESd, also showed significant changes ($P < 0.01$), reflecting ventricular remodeling in the model group. Stroke volume (SV) and heart rate (HR) did not differ significantly between the two groups. The HR values observed in our study fall within the normal physiological range previously reported for mice under comparable conditions, supporting the accuracy of the measurements. Using HE staining to examine myocardial morphology demonstrated that the CLP model significantly increased both cardiomyocyte cross-sectional area and interstitial fibrosis in the heart (Fig. 1B). Serum was collected 24 h after induction of the model. To determine the extent of sepsis-induced heart injury, we measured the expression levels of CK-MB, LDH, and cTnT in serum, all of which were overtly elevated by sepsis (Fig. 1C). All of these findings revealed that CLP was associated with cardiac dysfunction.

Identification and analysis of proteins

To gain a global view of DE proteins, we performed TMT labeled peptides to mark the proteins. In the CLP and Control (Ctr) groups, a total of 4,206 proteins were identified (Table S1). Of the 4206 proteins studied, 118 significantly changed between the CLP and the Ctr groups (Table S2). In comparison to the Ctr group, the CLP group showed an increase in 75 proteins and a decrease in 43 proteins (Fig. 2A). Using hierarchical cluster analysis, we were also able to locate proteins with similar levels of expression across various samples (Fig. 2B). To detect and classify the proteins related to their biological functions, we used a Gene Ontology (GO) analysis of 118 proteins and GO concepts tied to different proteins. In total, 118 GO terms were annotated, and the results of the studies revealed that 306 GO terms in biological processes (BP), 53 GO terms in cell components (CC), and 89 GO terms in molecular functions were significantly enriched (Fig. 2C). Blood microparticles, fibrinogen, intracellular ferritin, iron ion transport, and acute-phase response were among the GO keywords associated with these processes. In addition, to GO categorization, the proteins with the most significant differences in abundance were also annotated by KEGG (Fig. 2D). These pathways emerged directly from the significantly altered proteins and reflect inflammatory activation, coagulopathy, and iron-dependent stress processes associated with septic cardiomyopathy. Together, these enriched categories reflect known biological disturbances in septic cardiac injury. In particular, ferroptosis enrichment suggests enhanced lipid peroxidation and redox imbalance, whereas complement and coagulation cascades highlight the inflammatory and pro-thrombotic milieu characteristic of sepsis. We created a network of protein-protein interactions to show how the differently abundant proteins interact (Fig. 2E). An analysis of the network revealed the presence of several proteins that may be crucial to the SICM process, including the proteins Fgg, Fb, Fth1, Itih3, Serpin 3n, and Apob.

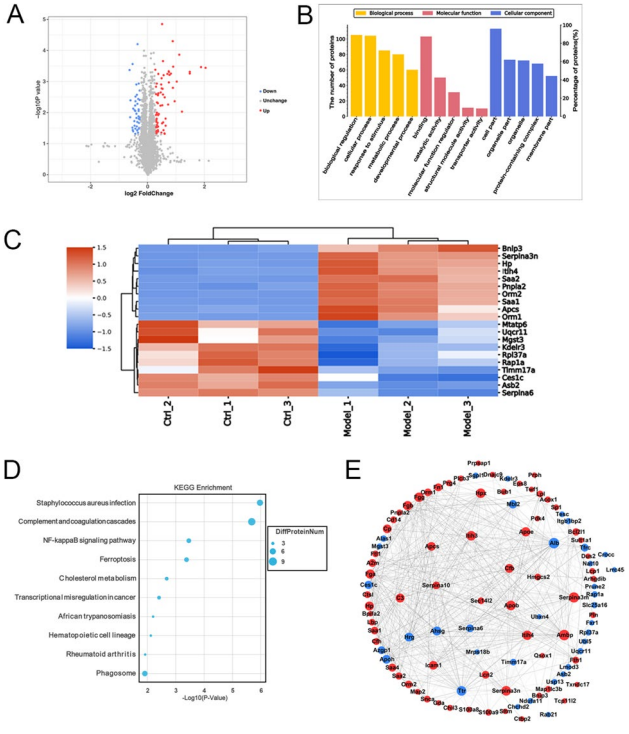

Fig. 2 The identification and analysis of differentially expressed proteins. **A** Depicts the volcano map. **B** The GO analysis. **C** The analysis of proteins using hierarchical clustering. **D** The KEGG analysis. **E** The protein-protein interaction (PPI) network analysis. The red color indicates the upregulated molecule, whereas the blue molecule represents the downregulated molecule

Identification and analysis of metabolites

Untargeted metabolomics using UHPLC-MS/MS technology was used to visualize cardiac tissues' metabolic profiles. The PCA offers valuable insights into the clustering and separation of two groups, which may potentially reflect a more effective outcome of the samples (Fig. 3A). The findings of the PLS-DA analysis indicated that the CLP and Ctr groups were segregated in both positive and negative modes, demonstrating an accurate illustration of the data and high probability. Additionally, permutation testing confirmed that the PLS-DA model did not overfit the data, indicating that septic cardiomyopathy resulted in significant metabolic differences across groups (Fig. 3B). Following that, a total of 190 DE metabolites were detected between the groups using the VIP ≥ 1 and fold change ≥ 1.5 and $p \leq 0.05$ criterion (Table S3). 174 metabolites were elevated, while 16 were downregulated (Fig. 3C). Additionally, metabolites annotated with MetaboAnalyst were primarily categorized as Linoleic acid metabolism, Taurine and hypotaurine metabolism, Phenylalanine metabolism, and Glycerophospholipid

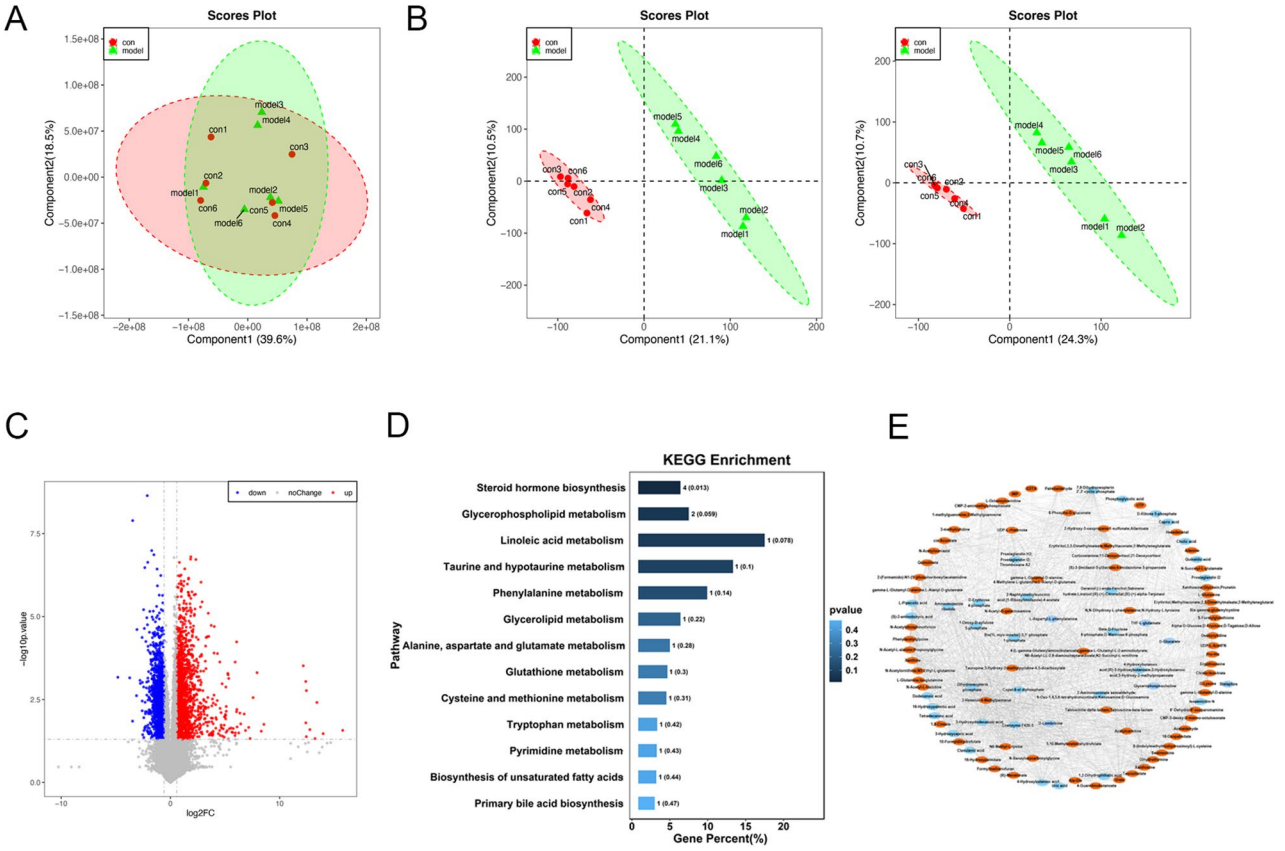

Fig. 3 Depicts the identification and analysis metabolites. **A** PCA, **B** Illustrates the PLS-DA for the models in the positive (left) and negative (right) ion modes. The CLP mice (green dots) and control mice (red dots) were categorized, and their hearts 2D were recorded. **C** The volcano map of metabolites. **D** KEGG analysis. **E** The metabolite-metabolite interaction network. The orange color indicates the upregulated metabolites, whereas the blue molecule represents the downregulated metabolites

metabolism (Fig. 3D). Moreover, to display the interaction of the metabolites, a network of metabolite-metabolite interactions was also created (Fig. 3E).

Integrated analysis of proteomics and metabolomics

To explore associations between metabolites and proteins, we generated loading plots of variables located in the joint component from both omics data. The loading number indicates the variable's ability to explain the difference between groups in each component, i.e., the degree to which the variable (metabolite/protein) contributes to the difference between groups (Fig. 4A). We analyzed cardiac tissues for DE proteins and DE metabolites to aid in the molecular interpretation of sepsis-induced cardiac failure. The top twenty common pathways between DE proteins and DE metabolites were identified (Table S4). Additionally, the shared pathway between DE proteins and DE metabolites was used to analyze the metabolite-transcript network (Fig. 4B). Significant changes ($P < 0.05$) in the pathway enrichment analysis of essential biological systems associated with platelet activation and mineral absorption. The enrichment of platelet activation pathways is consistent with sepsis-related endothelial activation and pro-coagulant signaling, further supporting the integrative findings. These proteins (Fgg, Fgb, Plcb3, Sp1, Acox1, etc.) may also play an essential role in these metabolites (Fig. 4C), as shown by a protein-metabolite interactions network (Prostaglandin H2, Prostaglandin I2, Thromboxane A2, 4-Hydroxybutanoic acid, Glycerophosphocholine, Citrate, Isocitrate, etc.).

Discussion

At present, no specific therapy is available for SICM. Elucidating the molecular characteristics of SICM therefore remains essential for understanding its pathophysiology and identifying potential therapeutic targets [13]. The pathophysiological causes of septic cardiomyopathy must be understood to develop a viable strategy for dealing with SICM and the rising septic death rate [14, 15]. Our research generated a sepsis mouse model based on echocardiography, heart morphology, and the expression of myocardial enzymes [16, 17]. The integrated proteomics and metabolomics investigation of septic cardiomyopathy tissues was confirmed based on the underlying mechanism in the protein-metabolite interaction pathway.

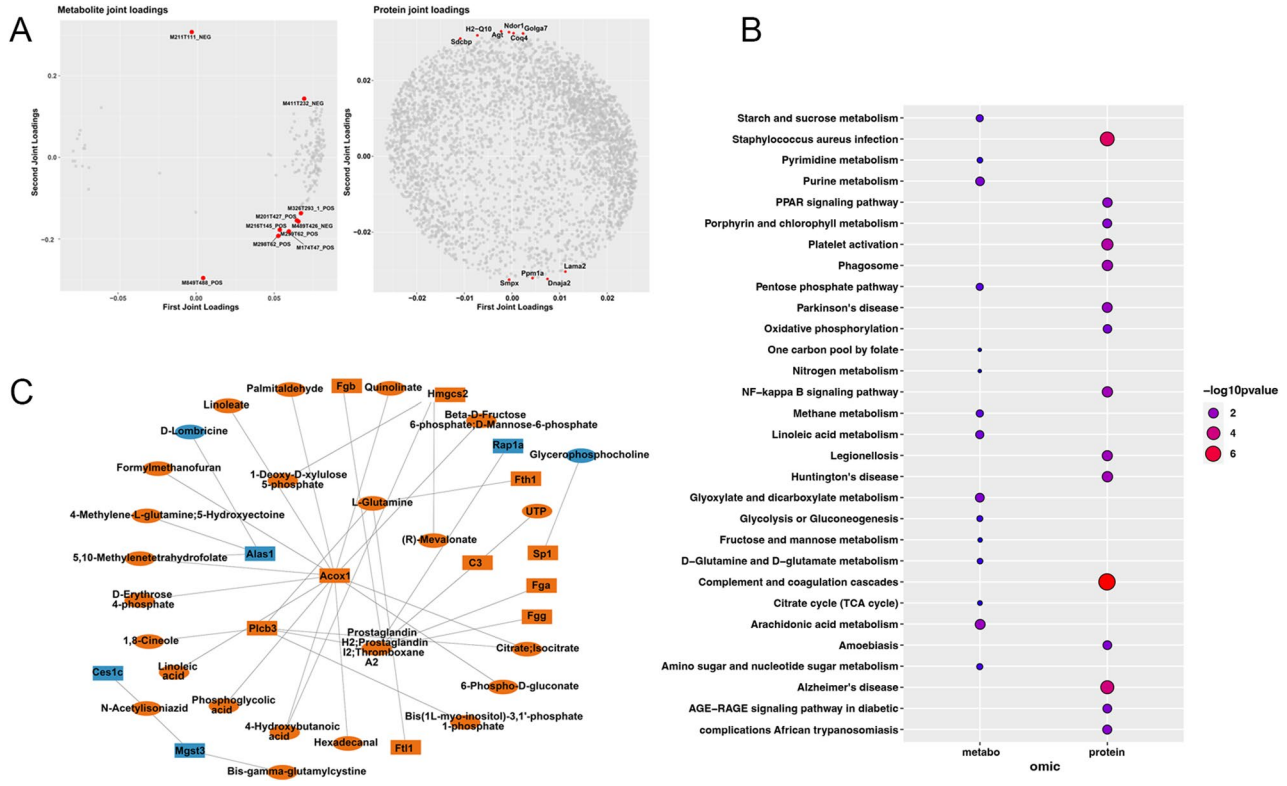

Fig. 4 Proteomics and metabolomics are being studied together. **A** Shows the loading plot of two omics. **B** Integrated KEGG analysis results of proteomics and metabolomics. **C** The routes were chosen as an intermediate carrier for the protein-metabolite interaction network, and the proteins and metabolites network were created. Proteins are represented by the circle, while metabolites are represented by the rectangle. The orange color indicates the upregulated proteins or metabolites, whereas the blue molecule represents the downregulated proteins or metabolites. The line number indicates that the proteins and metabolites are involved in multiple pathways

In this study, proteomic analysis identified 118 differentially expressed proteins in septic cardiac tissue, including increased levels of Snca, Prpsap1, Sp1, Qsox1, Lcp1, Arhgdib, Cfh, Gda, H1-3, and Prph. Notably, Prpsap1, Qsox1, and Prph proteins are three unique upregulated DE proteins that have not been described before. Prpsap1 has been implicated in nucleotide metabolism and cellular stress responses, suggesting a potential link to metabolic imbalance during sepsis. Qsox1, a known regulator of oxidative protein folding, may contribute to ER stress and redox dysregulation observed in septic myocardium. Prph, an intermediate filament protein traditionally associated with neuronal integrity, has recently been linked to cytoskeletal remodeling and cellular stress responses, raising the possibility that it participates in cardiomyocyte structural instability during sepsis. While these associations remain preliminary, they offer mechanistic hypotheses for future functional studies. Several of the identified proteins are mechanistically linked to pathways relevant to sepsis and inflammation. For example, Snca has been associated with impaired host defense and autophagic-lysosomal dysfunction during infection [18, 19]. Transcription factors such as Sp1 have been shown to mediate lipopolysaccharide-induced signaling through calcium and cAMP-dependent pathways and to regulate cardiomyocyte apoptosis [20, 21]. In addition, Cfh has been proposed as a possible biomarker in severe infectious states [22]. Together, these findings highlight a network of both known and novel proteins that may contribute to the pathogenesis of SICM.

Metabolomic analysis further demonstrated substantial metabolic reprogramming in septic cardiac tissue, consistent with the recognized role of metabolic dysregulation in cardiovascular disease and sepsis [23]. Alterations in amino acid metabolism and lipid-derived signaling molecules were prominent, supporting the concept that energy metabolism and inflammatory signaling are tightly coupled in septic myocardium. Although metabolic alterations such as glutamine depletion and lipid mediator dysregulation have been reported in systemic sepsis [24], their specific manifestation in cardiac tissue has been less well characterized. Our findings extend these observations by highlighting cardiac-specific metabolic signatures associated with SICM.

In terms of clinical relevance, several metabolites identified in our integrated analysis, particularly prostaglandin derivatives and L-glutamine, have been associated with inflammatory severity and metabolic recovery in

septic patients. Prostaglandin-related lipids reflect endothelial activation and platelet-vascular signaling, whereas L-glutamine depletion has been linked to impaired metabolic resilience in critical illness. These findings suggest potential translational value for risk stratification or metabolic monitoring in sepsis-related cardiac dysfunction. Our findings shed light on new ways in which platelet activation and mineral absorption may influence cardiac metabolism. Our integrated analysis identified several genes within protein–metabolite interaction networks that have not previously been associated with septic cardiomyopathy, including Fgg, Fgb, Rap1a, Plcb3, and TXA2. These factors are closely linked to platelet activation and inflammatory signaling, suggesting a potential role for platelet–cardiac crosstalk in septic myocardial dysfunction. Among them, Rap1a, a small GTPase that transduces extracellular stimuli into intracellular responses, has been shown to regulate inflammatory signaling and cardiac fibroblast activity [25–27]. Platelet activation during endotoxemia requires coordinated stimulation by agonists such as ADP, collagen, and TXA2 and has been reported to influence cardiac function by modulating leukocyte-endothelial interactions [28–30]. Collectively, these findings suggest coordinated interactions between proteins and their associated metabolites that may contribute to cardiac dysfunction in sepsis.

In conclusion, we sought to better understand septic cardiomyopathy by performing a protein-metabolite interaction investigation on cardiac tissues. The functional roles of network components suggest potential mechanistic contributions to cardiac metabolic alterations in sepsis, which merit further investigation. These findings demonstrate overlapping metabolic pathways affected in cardiac tissues and provide insight into the molecular changes associated with sepsis-induced heart dysfunction. Given the preclinical nature of this study, these results primarily offer mechanistic understanding rather than immediate clinical application. Once the relationship between the altered proteins/metabolites and the underlying pathophysiology of sepsis are established, this may inform future targeted investigations. Overall, our work contributes to the identification of novel biomarkers and lays a foundation for mechanistic studies in septic cardiomyopathy.

Limitations

This study has several limitations. First, the proteomic and metabolomic analyses were conducted with a relatively small number of biological replicates. Although the sample size meets commonly accepted standards for discovery-based sequencing studies, the findings should still be interpreted with appropriate caution. Second, while integrative multi-omics analyses identified multiple candidate molecules and pathways potentially involved in SICM, these findings remain largely descriptive and lack direct experimental validation. Future studies will be required to validate and functionally characterize the key molecular candidates identified here. Third, all validation work was performed in animals, since obtaining human cardiac tissue from septic patients is not feasible in practice. This limitation, while unavoidable, places certain constraints on direct clinical translation. Finally, although KEGG and GO pathway enrichment highlighted biologically meaningful processes such as ferroptosis and platelet activation, this study focused on reporting unbiased multi-omics results rather than providing in-depth mechanistic exploration, which should be addressed in future targeted studies.

Supplementary Information

The online version contains supplementary material available at https://doi.org/10.1186/s13104-026-07657-1.

Supplementary Material 1.

Supplementary Material 2.

Supplementary Material 3.

Supplementary Material 4.

Supplementary Material 5.

Acknowledgements

We wish to thank Xiaojin Wei, Ph.D. candidate at the Chinese Institute for Brain Research, for his invaluable assistance with statistical analysis and technical support.

Author contributions

Heyu Ji: Conceptualization, Methodology, Software, and Writing-Original draft. Ting Xiao: Data curation. Peijun Li: Visualization. Junmei Xu: Conceptualization and Supervision. Yulong Cui: Writing-Reviewing and Editing.

Funding

This study was supported by the National Natural Science Foundation of China (Grant No.81974018), and the National Key Research and Development Program of China (Grant No.2018YFC2001902).

Data availability

The raw proteomics and metabolomics data have been deposited in the ProteomeXchange Consortium via the PRIDE partner repository under the dataset identifier PXD030962. The data are publicly accessible and can be freely downloaded for reuse.

Declarations

Ethics approval and consent to participate

For this study, we secured ethics approval from the Institutional Animal Care and Use Committee at the Second Xiangya Hospital, which serves as the local animal care committee. This approval ensured compliance with ethical guidelines and standards for animal research. The study was carried out in compliance with the ARRIVE guidelines and the AVMA guidelines.

Consent for publication

Not applicable.

Competing interests

The authors declare no competing interests.

Received: 7 September 2025 / Accepted: 13 January 2026

Published online: 21 January 2026

References

1. Agor JK, Paramita N, Ozaltn OY. Prediction of sepsis related mortality: an optimization approach. IEEE J Biomed Health Inf. 2021;25(11):4207–16.
2. Rong J, Tao X, Lin Y, Zheng H, Ning L, Lu HS, Daugherty A, Shi P, Mullick AE, Chen S, et al. Loss of hepatic angiotensinogen attenuates Sepsis-Induced myocardial dysfunction. Circ Res. 2021;129(5):547–64.
3. Yamanashi T, Marra PS, Crutchley KJ, Wahba NE, Malicoat JR, Sullivan EJ, Akers CC, Nicholson CA, Herrmann FM, Karam MD, et al. Mortality among patients with sepsis associated with a bispectral electroencephalography (BSEEG) score. Sci Rep. 2021;11(1):14211.
4. Lee MT, Jung SY, Baek MS, Shin J, Kim WY, Early Vitamin C. Hydrocortisone, and Thiamine Treatment for Septic Cardiomyopathy: A Propensity Score Analysis. J Pers Med. 2021;11(7):610.
5. Rudiger A, Singer M. Mechanisms of sepsis-induced cardiac dysfunction. Crit Care Med. 2007;35(6):1599–608.
6. Geri G, Vignon P, Aubry A, Fedou AL, Charron C, Silva S, Repessé X, Vieillard-Baron A. Cardiovascular clusters in septic shock combining clinical and echocardiographic parameters: a post hoc analysis. Intensive Care Med. 2019;45(5):657–67.
7. Habimana R, Choi I, Cho HJ, Kim D, Lee K, Jeong I. Sepsis-induced cardiac dysfunction: a review of pathophysiology. Acute Crit Care. 2020;35(2):57–66.
8. Phillips DP, Kaynar AM. Septic cardiomyopathy. Int Anesthesiol Clin. 2012;50(3):187–201.
9. Liu DH, Ning YL, Lei YY, Chen J, Liu YY, Lin XF, Yang ZQ, Xian SX, Chen WT. Levosimendan versus Dobutamine for sepsis-induced cardiac dysfunction: a systematic review and meta-analysis. Sci Rep. 2021;11(1):20333.
10. Shao J, Pan T, Wang J, Tang T, Li Y, Jia X, Lai S. Integrated proteomics and metabolomics analysis of perirenal adipose tissue in obese rabbits treated with a restricted diet. Biology (Basel). 2021;10(4):321.
11. Chaudry IH, Wichterman KA, Baue AE. Effect of sepsis on tissue adenine nucleotide levels. Surgery. 1979;85(2):205–11.
12. Tan Y, Wan HH, Sun MM, Zhang WJ, Dong M, Ge W, Ren J, Peng H. Cardamonin protects against lipopolysaccharide-induced myocardial contractile dysfunction in mice through Nrf2-regulated mechanism. Acta Pharmacol Sin. 2021;42(3):404–13.
13. Bollen Pinto B, Ribas Ripoll V, Subías-Beltrán P, Herpain A, Barlassina C, Oliveira E, Pastorelli R, Braga D, Barcella M, Subirats L, et al. Application of an exploratory knowledge-discovery pipeline based on machine learning to multi-scale OMICS data to characterise myocardial injury in a cohort of patients with septic shock: an observational study. J Clin Med. 2021;10(19):4354.
14. Landesberg G, Gilon D, Meroz Y, Georgieva M, Levin PD, Goodman S, Avidan A, Beeri R, Weissman C, Jaffe AS, et al. Diastolic dysfunction and mortality in severe sepsis and septic shock. Eur Heart J. 2012;33(7):895–903.
15. Sturgess DJ, Marwick TH, Joyce C, Jenkins C, Jones M, Masci P, Stewart D, Venkatesh B. Prediction of hospital outcome in septic shock: a prospective comparison of tissue doppler and cardiac biomarkers. Crit Care. 2010;14(2):R44.
16. Hoffman M, Kyriazis ID, Lucchese AM, de Lucia C, Piedepalumbo M, Bauer M, Schulze PC, Bonios MJ, Koch WJ, Drosatos K. Myocardial strain and cardiac output are preferable measurements for cardiac dysfunction and can predict mortality in septic mice. J Am Heart Assoc. 2019;8(10):e012260.
17. Hollenberg SM, Singer M. Pathophysiology of sepsis-induced cardiomyopathy. Nat Rev Cardiol. 2021;18(6):424–34.
18. Tomlinson JJ, Shutinoski B, Dong L, Meng F, Elleithy D, Lengacher NA, Nguyen AP, Cron GO, Jiang Q, Roberson ED, et al. Holocranohistochemistry enables the visualization of α-synuclein expression in the murine olfactory system and discovery of its systemic anti-microbial effects. J Neural Transm (Vienna). 2017;124(6):721–38.
19. Mitroi DN, Karunakaran I, Gräler M, Saba JD, Ehninger D, Ledesma MD, van Echten-Deckert G. SGPL1 (sphingosine phosphate lyase 1) modulates neuronal autophagy via phosphatidylethanolamine production. Autophagy. 2017;13(5):885–99.
20. Liu W, Zhu ZQ, Wang W, Zu SY, Zhu GJ. Crucial roles of GATA-2 and SP1 in adrenomedullin-affected expression of tissue factor pathway inhibitor in human umbilical vein endothelial cells exposed to lipopolysaccharide. Thromb Haemost. 2007;97(5):839–46.
21. Chen DD, Wang HW, Cai XJ. Transcription factor Sp1 ameliorates sepsis-induced myocardial injury via ZFAS1/Notch signaling in H9C2 cells. Cytokine. 2021;140:155426.
22. Li J, Long D, Wu S, Wu X, Wei B, Chen D, Shao Y, Wang H, Cui L, Chen X, et al. Association of CFH polymorphism with susceptibility to sepsis caused by Pseudomonas aeruginosa in Chinese Han populations: A multi-center study. Gene. 2020;722:144127.
23. Chang P, Niu Y, Zhang X, Zhang J, Wang X, Shen X, Chen B, Yu J. Integrative proteomic and metabolomic analysis reveals metabolic phenotype in mice with Cardiac-Specific deletion of natriuretic peptide receptor A. Mol Cell Proteom. 2021;20:100072.
24. Poeze M, Luiking YC, Breedveld P, Manders S, Deutz NE. Decreased plasma glutamate in early phases of septic shock with acute liver dysfunction is an independent predictor of survival. Clin Nutr. 2008;27(4):523–30.
25. Yan J, Li F, Ingram DA, Quilliam LA. Rap1a is a key regulator of fibroblast growth factor 2-induced angiogenesis and together with Rap1b controls human endothelial cell functions. Mol Cell Biol. 2008;28(18):5803–10.
26. Wang H, Fotheringham L, Wittchen ES, Hartnett ME. Rap1 GTPase inhibits tumor necrosis Factor-α-Induced choroidal endothelial migration via NADPH Oxidase- and NF-κB-Dependent activation of Rac1. Am J Pathol. 2015;185(12):3316–25.
27. Burr SD, Stewart JA Jr. Rap1a regulates cardiac fibroblast contraction of 3D diabetic collagen matrices by increased activation of the AGE/RAGE cascade. Cells. 2021;10(6):1286.
28. Li RHL, Nguyen N, Tablin F. Canine platelets express functional Toll-like receptor-4: lipopolysaccharide-triggered platelet activation is dependent on adenosine diphosphate and thromboxane A2 in dogs. BMC Vet Res. 2019;15(1):245.
29. Nocella C, Carnevale R, Bartimoccia S, Novo M, Cangemi R, Pastori D, Calvieri C, Pignatelli P, Violi F. Lipopolysaccharide as trigger of platelet aggregation via eicosanoid over-production. Thromb Haemost. 2017;117(8):1558–70.
30. Loscalzo J, Welch G. Nitric oxide and its role in the cardiovascular system. Prog Cardiovasc Dis. 1995;38(2):87–104.

Publisher's note